Reduced order in domain control of distributed parameter port-Hamiltonian systems via energy shaping ⋆

Ning Liu [a], Yongxin Wu [b], Yann Le Gorrec [b], Laurent Lefevre [c], Hector Ramirez [d]

[a] *Université de Franche-Comté, SUPMICROTECH, CNRS, Institut FEMTO-ST, F-25000 Besançon, France*

[b] *SUPMICROTECH, CNRS, Institut FEMTO-ST, F-25000 Besançon, France*

[c] *Université Grenoble Alpes, LCIS, F-26902 Valence, France*

[d] *Universidad Tecnica Federico Santa Maria,Valparaiso, Chile*

Abstract

An in-domain finite dimensional controller for a class of distributed parameter systems on a one-dimensional spatial domain formulated under the port-Hamiltonian framework is presented. Based on (Trenchant et al. 2017) where positive feedback and a late lumping approach is used, we extend the Control by Interconnection method and propose a new energy shaping methodology with an early lumping approach on the distributed spatial domain of the system. Our two main control objectives are to stabilize the closed-loop system, as well as to improve the closed-loop dynamic performances. With the early lumping approach, we investigate two cases of the controller design, the ideal case where each distributed controller acts independently on the spatial domain (fully-actuated), and the more realistic case where the control action is piecewise constant over certain intervals (under-actuated). We then analyze the asymptotic stability of the closed-loop system when the infinite dimensional plant system is connected with the finite dimensional controller. Furthermore we provide simulation results comparing the performance of the fully-actuated case and the under-actuated case with an example of an elastic vibrating string.

Key words: Port-Hamiltonian systems; Distributed parameter systems; Passivity-based control; Casimir function; Optimization.

1 Introduction

The control of distributed parameter systems governed by partial differential equations (PDEs) has been the subject of an intensive research activity over the last decades [1,2]. Based on the location of actuators and sensors, control of PDEs is concerned with either boundary or in-domain distributed control. Typical in-domain distributed controls of PDEs have been investigated in [3] for nonlinear PDEs with non-normal linearizations, in [4,5] for optimal control, and in [6] for optimal control problem over a finite time interval, etc. Compared to the boundary control problems, this latter offers more degrees of freedom and can be extended to higher dimensional spatial domains where the input acts within the domain. In this paper, we focus on in-domain piecewise constant distributed control that allows to assign the dynamic performances over a given frequency range with clear physical interpretations. This piecewise constant in-domain control has been investigated in [7,8] using speed-gradient method. Different from the aforementioned approach, we design the controller on infinite dimensional port-Hamiltonian systems (PHSs), for its advantages in the modeling and possible extension to control of multi-physical nonlinear systems [9], which covers a wide domain of applications, such as fluid dynamics, chemical processes, and recently flexible structures actuated by soft actuators [10,11].

The concept of PHSs has firstly been introduced in the 90's in [12] for lumped parameter systems. It is an

⋆ This work has been supported by the EIPHI Graduate school (contract "ANR-17-EURE-0002") and the ANR Project IMPACTS (contract "ANR-21-CE48-0018") and ANID ECOS220040 project. The fifth author acknowledges Chilean FONDECYT 1191544 and CONICYT BASAL FB0008 projects. Corresponding author: Yongxin Wu.

Email addresses: ning.liu@femto-st.fr (Ning Liu), yongxin.wu@femto-st.fr (Yongxin Wu), yann.le.gorrec@ens2m.fr (Yann Le Gorrec), laurent.lefevre@lcis.grenoble-inp.fr (Laurent Lefevre), hector.ramireze@usm.cl (Hector Ramirez).

energy-based representation that expresses the power exchanges within the system and with its environment, using energy and co-energy variables and an intrinsic geometric structure, the Dirac structure. PHSs have later been extended to distributed parameter systems in [13]. The geometric Stokes-Dirac structure for linear distributed parameter PHSs defined on a one-dimensional (1D) spatial domain has been investigated in [14] using the semigroup theory. In terms of control, the Hamiltonian function is a good Lyapunov candidate function, and this class of systems exhibits an intrinsic passivity property, which makes passivity-based control (PBC) techniques suitable. Moreover, controllers designed through PBC have a clear physical interpretation. The PBC has been applied to lumped parameter PHSs and extensively studied in [15,16] leading to efficient control design techniques such as Control by Interconnection (CbI) and Interconnection and Damping Assignment (IDA)-PBC. [17] has generalized the CbI to distributed parameter PHSs with boundary control. The controller is designed to be a PHS. With the passive interconnection between the plant and the controller, the closed-loop system is again a PHS [16]. Casimir functions are then used to find an invariant relation between the state variables of the plant and those of the controller. By modifying the controller parameters, one can add damping to the closed-loop system (damping injection) and adjust the shape of its closed-loop Hamiltonian modifying both equilibrium and dynamic performances (energy shaping). The first result on CbI for distributed parameter PHSs with in-domain distributed control can be found in [18] where a positive feedback, late lumping approach and full actuation are investigated. Later on, [19] has applied the same late lumping approach, but with negative feedback and jet bundle formalism to design a finite dimensional port-Hamiltonian controller for piezo-actuated Euler-Bernoulli beam. The initial conditions have been estimated by an observer proposed in [20]. This controller has been extended to a 2D Kirchhoff–Love plate in [21]. Part of the controller state variables are used for energy shaping, whereas the others are for damping injection. As the jet bundle method focuses more on the geometric properties, the stability of the closed-loop system has not been investigated yet. Different from existing work in [18,19,21], we consider here the CbI of distributed PHS using a negative feedback, an early-lumping approach and a limited number of actuators. The controller design takes all the information of the discretized plant into account to achieve both energy shaping and damping injection at the same time.

The main contributions of this paper are:

(1) The generalization of the in-domain CbI established for the Timoshenko beam in [22] to a class of 1D linear distributed parameter PHSs which covers different physical applications such as vibrating strings, Timoshenko beams, Euler-Bernoulli beams, etc. With the early lumping approach, the finite dimensional controller is designed on the basis of the approximated finite dimensional plant system.
(2) Using the semigroup theory and passivity properties, we prove the asymptotic stability of the closed-loop system when the finite dimensional controller is applied to the infinite dimensional plant, getting rid of the well-known spillover effect [23].
(3) Besides the asymptotic stabilization of the closed-loop system, the controller improves the dynamic performances of the system over a given range of frequencies, *i.e.* accelerate the system with less oscillation and less overshoot.

Two different cases are investigated for the dynamic performances improvement: the ideal *fully-actuated case* where the control input works independently on each element of the discretized model and the *under-actuated case* where the input acts identically on sets of elements, providing less degrees of freedom. This latter case is closer to the real implementation because the control is usually carried out through actuator patches that act similarly over spatial elements. It is shown how to change the closed-loop energetic properties of the discretized system in a perfect way when the system is fully-actuated and in an *optimal way* when the system is under-actuated.

The paper is organized as follows: in Section 2 the port Hamiltonian formulation of a class of linear distributed parameter systems with two conservation laws and with in-domain control is presented, together with its structure-preserving discretization. The aforementioned CbI and energy shaping methods are investigated in Section 3 with a detailed closed-loop stability analysis. This control strategy takes advantage of the early lumping approach, leading to a directly implementable controller with guaranteed performances over a given frequency range. The passivity of the system and the damping injection guarantee the well-posedness and the asymptotic stability of the closed-loop system. Section 4 provides some simulation results with a comparison between the fully- and under-actuated cases using a vibrating string example, followed by the frequency analyses in Section 5. Section 6 ends up with conclusions and perspectives.

2 Port-Hamiltonian systems with in-domain control

In this paper, we consider partitioned port-Hamiltonian systems defined on a 1D spatial domain $\zeta \in [a, b]$ with distributed and boundary control and observation of the

form:

$$\frac{\partial}{\partial t}\begin{bmatrix} x_1(\zeta,t) \\ x_2(\zeta,t) \end{bmatrix} = \begin{bmatrix} 0 & \mathcal{G} \\ -\mathcal{G}^* & -R \end{bmatrix} \begin{bmatrix} \mathcal{L}_1(\zeta)x_1(\zeta,t) \\ \mathcal{L}_2(\zeta)x_2(\zeta,t) \end{bmatrix} \quad (1)$$

$$+ \begin{bmatrix} 0 \\ B_0 \end{bmatrix} u_d(\zeta,t), \quad (2)$$

$$y_d(\zeta,t) = \begin{bmatrix} 0 & B_0^T \end{bmatrix} \begin{bmatrix} \mathcal{L}_1(\zeta)x_1(\zeta,t) \\ \mathcal{L}_2(\zeta)x_2(\zeta,t) \end{bmatrix}, \quad (3)$$

$$u_b = \mathcal{B}\begin{bmatrix} \mathcal{L}_1(\zeta)x_1(\zeta,t) \\ \mathcal{L}_2(\zeta)x_2(\zeta,t) \end{bmatrix}, y_b = \mathcal{C}\begin{bmatrix} \mathcal{L}_1(\zeta)x_1(\zeta,t) \\ \mathcal{L}_2(\zeta)x_2(\zeta,t) \end{bmatrix}, \quad (4)$$

where $x = [x_1^T, x_2^T]^T \in X := L^2([a,b],\mathbb{R}^n) \times L^2([a,b],\mathbb{R}^n)$, $\mathcal{L} = \text{diag}(\mathcal{L}_1, \mathcal{L}_2)$ is a bounded and Lipschitz continuous matrix-valued function such that $\mathcal{L}(\zeta) = \mathcal{L}^T(\zeta)$ and $\mathcal{L}(\zeta) \geq \eta$ with $\eta > 0$ for all $\zeta \in [a,b]$. The dissipation operator R is bounded, symmetric ($R^* = R$) and coercive ($\langle z, Rz\rangle_{L_2} > c\|z\|_{L_2}$, $\forall z \in L_2([a,b],\mathbb{R}^n)$ and $c > 0$). $\mathcal{B}(\cdot)$ and $\mathcal{C}(\cdot)$ are some boundary input and boundary output mapping operators that will be defined later. $B_0 \in \mathbb{R}^{n\times 1}$ is full rank. $X \ni x$ is the space of energy variables and $\mathcal{L}x$ denotes the co-energy variables associated to the energy variables x. The total energy of the system is given by:

$$H(x_1,x_2) = \frac{1}{2}\int_a^b \Big(\mathcal{L}_1(\zeta)x_1^2(\zeta,t) + \mathcal{L}_2(\zeta)x_2^2(\zeta,t)\Big)\,\mathrm{d}\zeta. \quad (5)$$

Furthermore, we consider in this paper that:

$$\mathcal{G} = G_0 + G_1\frac{\partial}{\partial\zeta}, \quad (6)$$

with $G_0, G_1 \in \mathbb{R}^{n\times n}$ and G_1 full rank. $\mathcal{G}^*$ is the formal adjoint of $\mathcal{G}$ *i.e.*

$$\mathcal{G}^* = G_0^T - G_1^T\frac{\partial}{\partial\zeta}.$$

u_d and y_d denote the distributed input and output, respectively. The system (1-4) with (6) stems from the modeling of flexible structures like elastic strings, waves or Timoshenko beams and beams organised in networks. The distributed input which is applied only to x_2 can be considered as an exerted force/torque. The proposed approach is easy to extend to second order operators defining Euler-Bernoulli beam equation for example.

We define $P_1 = \begin{bmatrix} 0 & G_1 \\ G_1^T & 0 \end{bmatrix}$.

Definition 1 *The boundary port variables associated to the system* (1) *are defined by:*

$$\begin{bmatrix} f_\partial \\ e_\partial \end{bmatrix} = \underbrace{\frac{1}{\sqrt{2}}\begin{bmatrix} P_1 & -P_1 \\ I & I \end{bmatrix}}_{R_{ext}} \begin{bmatrix} \mathcal{L}x(b) \\ \mathcal{L}x(a) \end{bmatrix}. \quad (7)$$

By definition the boundary port variables result to:

$$\frac{\mathrm{d}H}{\mathrm{d}t} = \int_a^b y_d^* u_d\,\mathrm{d}\zeta + f_\partial^T e_\partial - \int_a^b (\mathcal{L}_2 x_2)^* R(\mathcal{L}_2 x_2)d\zeta. \quad (8)$$

Theorem 1 *Let W be a $2n \times 4n$ matrix. If W has full rank and satisfies $W\boldsymbol{\Sigma}W^T \geq 0$, where $\boldsymbol{\Sigma} = \begin{bmatrix} 0 & I \\ I & 0 \end{bmatrix}$, then the system operator*

$$\mathcal{A} = (\mathcal{J} - \mathcal{R})\,\mathcal{L},$$

where

$$\mathcal{J} = \begin{bmatrix} 0 & \mathcal{G} \\ -\mathcal{G}^* & 0 \end{bmatrix} \text{ and } \mathcal{R} = \begin{bmatrix} 0 & 0 \\ 0 & R \end{bmatrix}$$

with domain

$$D(\mathcal{A}) = \left\{ x \in H^1\left([a,b],\mathbb{R}^{2n}\right) \mid \begin{bmatrix} f_\partial \\ e_\partial \end{bmatrix} \in ker(W) \right\}$$

generates a contraction semigroup on X.

PROOF. The proof follows Theorem 4.1 in [14].

Boundary inputs and outputs are defined by:

$$u_b = W\begin{bmatrix} f_\partial^T & e_\partial^T \end{bmatrix}^T, \quad y_b = \tilde{W}\begin{bmatrix} f_\partial^T & e_\partial^T \end{bmatrix}^T. \quad (9)$$

With the plant system established, the first step in the design procedure using an early lumping approach is to spatially discretize (1). The discretization needs to preserve both the Dirac structure and the passivity of the system to take advantage of the PHS properties. Therefore we apply the mixed finite element method [24], and the approximated system of (1) is again a PHS with

p elements:

$$\begin{bmatrix} \dot{x}_{1d} \\ \dot{x}_{2d} \end{bmatrix} = (J_n - R_n) \begin{bmatrix} Q_1 x_{1d} \\ Q_2 x_{2d} \end{bmatrix} + B_b u_b + \begin{bmatrix} 0 \\ B_{0d} \end{bmatrix} \mathbf{u}_d, \tag{10a}$$

$$y_b = B_b^T \begin{bmatrix} Q_1 x_{1d} \\ Q_2 x_{2d} \end{bmatrix} + D_b u_b, \tag{10b}$$

$$\mathbf{y}_d = \begin{bmatrix} 0 & B_{0d}^T \end{bmatrix} \begin{bmatrix} Q_1 x_{1d} \\ Q_2 x_{2d} \end{bmatrix}, \tag{10c}$$

where $x_{id} = \begin{bmatrix} x_i^1 & \cdots & x_i^p \end{bmatrix}^T$ for $i \in \{1, \cdots, 2n\}$, $\mathbf{u}_d \in \mathbb{R}^p$, $\mathbf{y}_d \in \mathbb{R}^p$,

$$J_n = \begin{bmatrix} 0 & J_i \\ -J_i^T & 0 \end{bmatrix} \quad \text{and} \quad R_n = \begin{bmatrix} 0 & 0 \\ 0 & R_d \end{bmatrix},$$

are the discretized matrices of the operators $\mathcal{J}$ and $\mathcal{R}$ with J_i and R_d the discretized matrices of the operators $\mathcal{G}$ and R. $Q_1 \in \mathbb{R}^{np \times np}$ and $Q_2 \in \mathbb{R}^{np \times np}$ are the discretized matrices of $\mathcal{L}_1$ and $\mathcal{L}_2$, respectively. $B_{0d} \in \mathbb{R}^{np \times p}$ is the discretization of the input mapping B_0 over the spatial domain.

The input u_b denotes the boundary input which corresponds to the boundary actuation or/and conditions. Since the distributed actuation of the system is considered, we assume that there is no energy changes (actuation) at the boundary of the spatial domain, *i.e.* $u_b = 0$ and the discretized system (10) can therefore be simplified.

The Hamiltonian of the discretized model (10) writes:

$$H_d(x_{1d}, x_{2d}) = \frac{1}{2} \left(x_{1d}^T Q_1 x_{1d} + x_{2d}^T Q_2 x_{2d} \right). \tag{11}$$

It is important to notice that in what follows the choice of the structure-preserving discretization method is not unique. One could have alternatively used other discretization methods such as [25,26] that also guarantee the existence of port-Hamiltonian structure and structural invariants suitable for control design purposes. Furthermore, we consider a finite number of inputs for control design. In this regard, the infinite dimensional system (1) is in general not controllable but stabilizable, because the uncontrollable modes are already exponentially stable.

3 Control by interconnection and energy shaping

In this section, we extend the CbI method to the in-domain distributed input and output case. The main difference with CbI for finite dimensional PHSs [15,16] is that the controller takes the overall information of the plant into consideration, as depicted in Fig. 1 for an ideal interconnection case. The arrows in Fig. 1 represent the signals of both input and output. $\mathbf{u}_d$ and $\mathbf{y}_d$ represent the power conjugated distributed input and output of system (10). u_c and y_c are power conjugated input and output of the controller (12). These two pairs of input and output are interconnected in a power-preserving way as formulated in (13). As a result, one can shape the distributed Hamiltonian function all over the system with an appropriate parametrization of the controller and the use of structural invariants *i.e.* Casimir functions [9]. The main objective of the proposed CbI method is to improve the closed-loop performances over a given frequency range while guaranteeing the overall closed-loop stability (v.s. neglected dynamics during the synthesis). One can also modify the equilibrium point by changing the minima of the energy function.

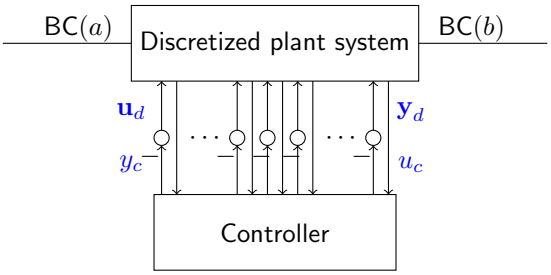

Fig. 1. Distributed control by interconnection strategy.

The controller in Fig. 1 is designed to be a finite dimensional PHS, which is expressed as follows:

$$\begin{aligned} \dot{x}_c &= (J_c - R_c) Q_c x_c + B_c u_c, \\ y_c &= B_c^T Q_c x_c + D_c u_c, \end{aligned} \tag{12}$$

where $x_c \in \mathbb{R}^m$, $J_c = -J_c^T \in \mathbb{R}^{m \times m}$, $R_c = R_c^T \geq 0$ and $Q_c = Q_c^T \geq 0$, $B_c \in \mathbb{R}^{m \times m}$, $\mathbb{R}^{m \times m} \ni D_c \geq 0$, $u_c \in \mathbb{R}^m$ and $y_c \in \mathbb{R}^m$. Matrices Q_c and D_c are used for energy shaping and damping injection/diffusion, respectively.

Without considering external signals, the interconnection between the discretized plant system (10) and the controller (12) is given by

$$\begin{bmatrix} \mathbf{u}_d \\ u_c \end{bmatrix} = \begin{bmatrix} 0 & -M \\ M^T & 0 \end{bmatrix} \begin{bmatrix} \mathbf{y}_d \\ y_c \end{bmatrix}, \tag{13}$$

where $\mathbb{R}^{p \times m} \ni M = I_m \otimes \mathbf{1}_k$, with I_m the identity matrix of dimension m, $\mathbf{1}_k$ a ones vector of dimension $k \times 1$, and

$\otimes$ denoting the Kronecker product. k is the number of elements covered by one actuator. The relation between m, k and p is given by:

$$p = mk.$$

The passive interconnection (13) guarantees the passivity of the closed-loop system. It results in a new PHS in closed-loop:

$$\dot{x}_{cl} = (J_{cl} - R_{cl})\, Q_{cl} x_{cl}, \tag{14}$$

where $x_{cl} = \left[x_{1d}^T,\, x_{2d}^T,\, x_c^T\right]^T$, $Q_{cl} = \text{diag}\left(Q_1,\, Q_2,\, Q_c\right)$,

$$J_{cl} = \begin{bmatrix} 0 & J_i & 0 \\ -J_i^T & 0 & -B_{0d} M B_c^T \\ 0 & B_c M^T B_{0d}^T & J_c \end{bmatrix},$$

$$R_{cl} = \begin{bmatrix} 0 & 0 & 0 \\ 0 & R_d + B_{0d} M D_c M^T B_{0d}^T & 0 \\ 0 & 0 & R_c \end{bmatrix}.$$

The Hamiltonian of the controller (12) is:

$$H_c(x_c) = \frac{1}{2} x_c^T Q_c x_c. \tag{15}$$

Therefore, the closed-loop Hamiltonian function reads:

$$H_{cld}(x_{1d}, x_{2d}, x_c) = H_d(x_{1d}, x_{2d}) + H_c(x_c). \tag{16}$$

The next step is to design the controller matrices J_c, R_c, B_c, Q_c, and D_c in order to shape the closed-loop Hamiltonian (16). In Proposition 1 we first show how the controller states can be related to the plant states using structural invariants.

Proposition 1 *The closed-loop system* (14) *admits the Casimir function* $C(x_{1d}, x_c)$ *defined by:*

$$C(x_{1d}, x_c) = B_c M^T B_{0d}^T J_i^{-1} x_{1d} - x_c \tag{17}$$

as structural invariant, i.e. $\dot{C}(x_{1d}, x_c) = 0$ *along the closed-loop trajectories, as soon as* J_c *and* R_c *are chosen equal to zero. If the initial conditions of* $x_{1d}(0)$ *and* $x_c(0)$ *satisfy* $C(x_{1d}(0), x_c(0)) = 0$*, the controller is a proportional-integral control, and the control law* (12)-(13) *is equivalent to the state feedback:*

$$\begin{aligned} y_c &= B_c^T Q_c B_c M^T B_{0d}^T J_i^{-1} x_{1d} + D_c M^T B_{0d}^T Q_2 x_{2d}, \\ \mathbf{u}_d &= -M y_c. \end{aligned} \tag{18}$$

Therefore, the closed-loop system yields:

$$\begin{bmatrix} \dot{x}_{1d} \\ \dot{x}_{2d} \end{bmatrix} = \begin{bmatrix} 0 & J_i \\ -J_i^T & -\tilde{R}_d \end{bmatrix} \begin{bmatrix} \tilde{Q}_1 x_{1d} \\ Q_2 x_{2d} \end{bmatrix}, \tag{19}$$

where

$$\tilde{R}_d = R_d + B_{0d} M D_c M^T B_{0d}^T, \tag{20}$$

$$\tilde{Q}_1 = Q_1 + J_i^{-T} B_{0d} M B_c^T Q_c B_c M^T B_{0d}^T J_i^{-1}, \tag{21}$$

are the new closed-loop dissipation matrix and energy matrix associated to x_{1d}*.*

PROOF. We consider here Casimir functions of the form:

$$C(x_{1d}, x_{2d}, x_c) = F(x_{1d}, x_{2d}) - x_c. \tag{22}$$

The time derivative of C is given by

$$\begin{aligned} \frac{\mathrm{d}C}{\mathrm{d}t} &= \frac{\partial^T C}{\partial x_{cl}} \frac{\partial x_{cl}}{\partial t} \\ &= \left[\tfrac{\partial^T F}{\partial x_{1d}},\, \tfrac{\partial^T F}{\partial x_{2d}},\, -I\right] (J_{cl} - R_{cl})\, e_{cl}, \end{aligned} \tag{23}$$

where $e_{cl} = \frac{\partial H_{cld}}{\partial x_{cl}} = Q_{cl} x_{cl}$. The Casimir functions are dynamic invariants, *i.e.* $\dot{C} = 0$ that do not depend on the trajectories of the system (which is related to the Hamiltonian). Therefore, (23) with $\dot{C} = 0$ gives rise to the following matching equations:

$$\frac{\partial^T F}{\partial x_{2d}} \left(-J_i^T\right) = 0, \tag{24a}$$

$$\frac{\partial^T F}{\partial x_{1d}} J_i - \frac{\partial^T F}{\partial x_{2d}} \tilde{R}_d - B_c M^T B_{0d}^T = 0, \tag{24b}$$

$$\frac{\partial^T F}{\partial x_{2d}} \left(-B_{0d} M B_c^T\right) - (J_c - R_c) = 0. \tag{24c}$$

Solving (24a), one gets $\partial F / \partial x_{2d} = 0$, which indicates that x_c does not depend on x_{2d}. Therefore, with $J_c = -J_c^T$ and $R_c = R_c^T \geq 0$, (24c) indicates that J_c and R_c equal zero. Since J_i is full rank, from (24b) one gets (17) as a structural invariant as soon as the initial condition $x_c(0)$ is chosen properly. Taking the initial conditions $x_{1d}(0)$ and $x_c(0)$ such that $C(x_{1d}(0), x_c(0)) = 0$, (17) becomes:

$$B_c M^T B_{0d}^T J_i^{-1} x_{1d}(t) - x_c(t) = 0, \tag{25}$$

which allows to link the state of the controller with the state of the plant. Replacing x_c in (14) by (25), the control law (12) becomes a state feedback as formulated in (18). Therefore the closed-loop system (14) becomes (19).

Remark 1 *The choice of Casimir function is in general not unique. Yet considering the fact that both system and controller are linear and the fact that Casimir functions are structural invariants that should not depend on the Hamiltonian, the set of possible Casimir functions reduces to linear functions of the form* (22)*.*

From Proposition 1, the closed-loop Hamiltonian function (16) is now only a function of the discretized plant state variables:

$$H_{cld}(x_{1d}, x_{2d}) = \frac{1}{2}\left(x_{1d}^T \tilde{Q}_1 x_{1d} + x_{2d}^T Q_2 x_{2d}\right), \quad (26)$$

with its time derivative being:

$$\frac{\mathrm{d}H_{cld}}{\mathrm{d}t} = -x_{2d}^T Q_2 \tilde{R}_d Q_2 x_{2d} \leq 0. \quad (27)$$

From a physical point of view, (26) implies that with the dynamic controller (12) equivalent to the state feedback (18), it is possible to change, at least partially (depending on p and the range of B_{0d}), the energy matrix related to x_{1d}. For a given number of distributed input m, the objectives of the energy shaping is to look for matrices B_c and Q_c such that the norm of the difference (considered here in the Frobenius norm, see Definition 6.4 of [27]) between the desired energy matrix $\tilde{Q}_{1d}$ and the closed-loop one $\tilde{Q}_1$ is minimal:

$$\min_{B_c^T Q_c B_c} \left\| \underbrace{J_i^{-T} B_{0d} M B_c^T Q_c B_c M^T B_{0d}^T J_i^{-1} + Q_1}_{\tilde{Q}_1} - \tilde{Q}_{1d} \right\|_F . \quad (28)$$

Actually, because $B_{0d} \in \mathbb{R}^{np \times p}$ and from the definition of $\tilde{Q}_1$ in equation (21), one can only shape independently the energy matrix related to p elements of x_{1d}. Therefore, by multiplying B_{0d}^T and B_{0d} on both sides of matrices inside the Frobenius norm, (28) can be simplified as:

$$\min_{B_c^T Q_c B_c} \left\| B_{0d}^T J_i^{-T} B_{0d} M B_c^T Q_c B_c M^T B_{0d}^T J_i^{-1} B_{0d} - Q_m \right\|_F \quad (29)$$

with $\mathbb{R}^{p\times p} \ni Q_m = B_{0d}^T \left(\tilde{Q}_{1d} - Q_1\right) B_{0d}$ full rank and $Q_m \geq 0$ [1]. Furthermore (29) can be formalized by the optimization Problem 1.

Problem 1 *The closed-loop energy function related to p elements of x_{1d} is shaped in an optimal way if and only if $\boldsymbol{X} = B_c^T Q_c B_c \in SR_0^{m\times m}$ minimizes the criterion*

$$f(\boldsymbol{X}) = \left\| A \boldsymbol{X} A^T - Q_m \right\|_F , \quad (30)$$

where $A = B_{0d}^T J_i^{-T} B_{0d} M \in \mathbb{R}^{p\times m}$ and $SR_0^{m\times m}$ represents the set of symmetric and positive semi-definite matrices.

The solution to Problem 1 depends on the independent number of distributed input that are available. We consider two different cases: the *ideal* fully-actuated case ($m = p$) and the under-actuated case ($m < p$).

3.1 Fully-actuated case

We first consider the fully-actuated case where each discretized element of the plant is controlled by an independent input, *i.e.* $\mathbf{u}_d \in \mathbb{R}^m$ and $m = p$, as illustrated in Fig. 2. The input matrix $M = I \in \mathbb{R}^{p\times p}$. Therefore, the

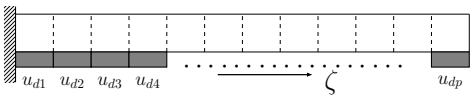

Fig. 2. Fully-actuated case illustration.

optimization Problem 1 admits an exact solution that is given in Proposition 2.

Proposition 2 *In the fully-actuated case, i.e. $m = p$ the optimization Problem 1 has an exact analytical solution $\hat{\boldsymbol{X}} = \left(B_{0d}^T J_i^{-T} B_{0d}\right)^{-1} Q_m \left(B_{0d}^T J_i^{-1} B_{0d}\right)^{-1}$ leading to $f(\boldsymbol{X}) = 0$. The controller matrices B_c and Q_c can be chosen as:*

$$B_c = \left(B_{0d}^T J_i^{-1} B_{0d}\right)^{-1}, \quad Q_c = Q_m. \quad (31)$$

PROOF. With M being the identity matrix, the matrix $\mathbb{R}^{p\times p} \ni A = B_{0d}^T J_i^{-T} B_{0d}$ is invertible. Therefore, (30) admits a minimum in 0 when:

$$\begin{aligned} \hat{\boldsymbol{X}} &= A^{-1} Q_m A^{-T} \\ &= \left(B_{0d}^T J_i^{-T} B_{0d}\right)^{-1} Q_m \left(B_{0d}^T J_i^{-1} B_{0d}\right)^{-1}. \end{aligned} \quad (32)$$

From the expression of $\boldsymbol{X}$, one can choose B_c and Q_c as in (31) to satisfy (32).

3.2 Under-actuated case

We study now the more realistic case where the same control input is applied to a set of elements, as shown in Fig. 3, where k denotes the number of elements sharing

[1] Q_m can be either positive semi-definite, or negative semi-definite with some restrictions to guarantee a stable closed-loop system, depending on the fact that one wants to increase or decrease the closed-loop stiffness. In order to improve the closed-loop performances we consider the former case, i.e. $Q_m \geq 0$.

the same input. The number of distributed inputs m is less than the number of discretized elements p, and follows $m = p/k$.

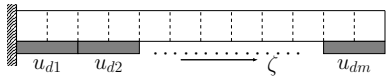

Fig. 3. Under-actuated case with an example of $k = 2$.

In this case the controller has less degrees of freedom than in the fully actuated case, hence the matrix $A \in \mathbb{R}^{p\times m}$ in (30) is not invertible and the optimization Problem 1 is ill-conditioned. The solution of the optimization Problem 1 is given in Proposition 3.

Proposition 3 *$f(\boldsymbol{X})$ defined in (30) is convex and the minimization of $f(\boldsymbol{X})$ is equivalent to the minimization of $f^2(\boldsymbol{X})$, which has a unique minimum given for $\hat{\boldsymbol{X}} = V\Sigma_0^{-1}U_1^T Q_m U_1 \Sigma_0^{-1} V^T$, with V, Σ_0 and U_1 the matrices of the singular value decomposition of the matrix A i.e.*

$$A = U\Sigma V^T = \begin{bmatrix} U_1 & U_2 \end{bmatrix} \begin{bmatrix} \Sigma_0 \\ 0 \end{bmatrix} V^T, \tag{33}$$

where $U \in \mathbb{R}^{p\times p}$ and $V \in \mathbb{R}^{m\times m}$ are unitary matrices, $U_1 \in \mathbb{R}^{p\times m}$, $U_2 \in \mathbb{R}^{p\times(p-m)}$, and $\Sigma_0 = \Sigma_0^T \geq 0$ is the diagonal matrix composed of singular values of A.

PROOF. The proof of Proposition 3 is similar to that of Proposition 3 in [22]. Substituting (33) into $f^2(\boldsymbol{X})$, one gets:

$$\begin{aligned}
&\min_{\boldsymbol{X}\in SR_0^{m\times m}} f^2(\boldsymbol{X}) \\
&= \min_{\boldsymbol{X}\in SR_0^{m\times m}} \left\| U\Sigma V^T \boldsymbol{X} V \Sigma^T U^T - Q_m \right\|_F^2 \\
&= \min_{\boldsymbol{X}\in SR_0^{m\times m}} \left(\left\| \Sigma_0 V^T \boldsymbol{X} V \Sigma_0^T - T_1 \right\|_F^2 + 2\|T_2\|_F^2 + \|T_3\|_F^2 \right),
\end{aligned} \tag{34}$$

where $T_1 = U_1^T Q_m U_1$, $T_2 = U_1^T Q_m U_2$, and $T_3 = U_2^T Q_m U_2$. Since $\|T_2\|_F^2$ and $\|T_3\|_F^2$ are given once the matrices A and Q_m are defined, the minimization of (34) is equivalent to:

$$\min_{\bar{\boldsymbol{X}}\in SR_0^{m\times m}} \left\| \bar{\boldsymbol{X}} - T_1 \right\|_F^2, \text{ with } \bar{\boldsymbol{X}} = \Sigma_0 V^T \boldsymbol{X} V \Sigma_0^T. \tag{35}$$

According to Theorem 2.1 in [28], $T_1 \in SR_0^{m\times m}$, and (35) admits a unique solution $\hat{\bar{\boldsymbol{X}}} = T_1$. Therefore, (34) has the minimum when:

$$\hat{\boldsymbol{X}} = V\Sigma_0^{-1}\hat{\bar{\boldsymbol{X}}}\Sigma_0^{-1}V^T = V\Sigma_0^{-1}U_1^T Q_m U_1 \Sigma_0^{-1} V^T. \tag{36}$$

The choice of controller matrices B_c and Q_c is not unique, as long as they satisfy the condition (36). We will present a possible choice in Subsection 4.2.

Remark 2 *We have investigated the choices of controller matrices B_c and Q_c under two different cases in Proposition 2 and 3, respectively. The objective is to shape the closed-loop Hamiltonian H_{cld} with the modification of part of the potential energy matrix. The choice of the controller matrix D_c follows the similar procedure, with the optimization of the difference between (27) and the desired one.*

3.3 Closed-loop stability

In this subsection we consider the closed-loop stability of the infinite-dimensional system (1) controlled by the finite-dimensional controller (12) derived from the early lumping approach. The power-preserving interconnection between (1) and (12) is formulated as:

$$\begin{bmatrix} u_d \\ u_c \end{bmatrix} = \begin{bmatrix} 0 & -\mathbf{1}_\zeta \\ \mathbf{1}_\zeta^* & 0 \end{bmatrix} \begin{bmatrix} y_d \\ y_c \end{bmatrix}, \tag{37}$$

with

$$\mathbf{1}_\zeta : \mathbb{R}^m \to L_2, \qquad \mathbf{1}_\zeta^* : L_2 \to \mathbb{R}^m. \tag{38}$$

$\mathbf{1}_\zeta$ is the characteristic function that distributes the point-wise value of the controller in $\mathbb{R}^m$ space to the sub-interval L_2 space, as illustrated in Fig. 4.

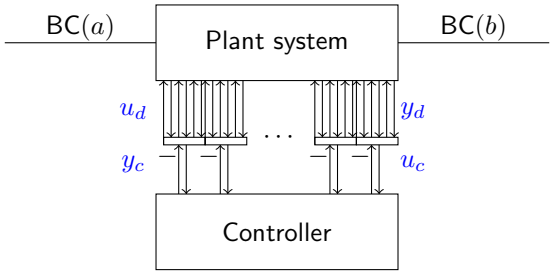

Fig. 4. Distributed control by interconnection strategy.

Lemma 1 *The interconnection (37) generates a Dirac structure with the following power conservation:*

$$\int_a^b y_d^* \mathbf{1}_\zeta y_c \, \mathrm{d}\zeta = y_c^T \mathbf{1}_\zeta^* y_d. \tag{39}$$

The closed-loop system is equivalent to:

$$\dot{\mathcal{X}} = \underbrace{\begin{bmatrix} 0 & \mathcal{G} & 0 \\ -\mathcal{G}^* & -\mathcal{R}_{cl} & -B_0\mathbf{1}_\zeta B_c^T \\ 0 & B_c\mathbf{1}_\zeta^* B_0^* & 0 \end{bmatrix}}_{\mathcal{A}_{cl}} \mathcal{L}_{cl}\,\mathcal{X}, \tag{40}$$

where $\mathcal{X} = \begin{bmatrix} x \\ x_c \end{bmatrix} \in X_s$ is the state defined on the state space $X_s = L_2\left([a,b],\mathbb{R}^{2n}\right) \times \mathbb{R}^m$, $\mathcal{R}_{cl} = R + B_0\mathbf{1}_\zeta D_c \mathbf{1}_\zeta^* B_0^*$ and $\mathcal{L}_{cl} = \mathrm{diag}\,(\mathcal{L}_1, \mathcal{L}_2, Q_c)$. The domain of $\mathcal{A}_{cl}$ is defined as:

$$D\left(\mathcal{A}_{cl}\right) = \left\{ \mathcal{X} \in H^1\left([a,b],\mathbb{R}^{2n}\right) \times \mathbb{R}^m, \mathcal{B}\left(\mathcal{L}x\right) = 0 \right\}.$$

The Hamiltonian of (40) is:

$$H_{cl} = \frac{1}{2}\int_a^b \left(\mathcal{L}_1(\zeta)x_1^2(\zeta,t) + \mathcal{L}_2(\zeta)x_2^2(\zeta,t)\right)\mathrm{d}\zeta + \frac{1}{2}x_c^T Q_c x_c \tag{41}$$

with

$$\begin{aligned} \frac{\mathrm{d}H_{cl}}{\mathrm{d}t} &= \int_a^b y_d^* u_d\,\mathrm{d}\zeta + y_c^T u_c - \int_a^b (\mathcal{L}_2 x_2)^* \mathcal{R}_{cl}(\mathcal{L}_2 x_2) d\zeta \\ &= -\int_a^b (\mathcal{L}_2 x_2)^* \mathcal{R}_{cl}(\mathcal{L}_2 x_2) d\zeta. \end{aligned} \tag{42}$$

The last step of (42) is derived considering (39).

In order to prove the stability of the closed-loop system using Lyapunov arguments and LaSalle's invariance principle, we first state the following theorems.

Theorem 2 *The linear operator $\mathcal{A}_{cl}$ defined in* (40) *generates a contraction semigroup on X_s.*

PROOF. To prove that the closed-loop operator $\mathcal{A}_{cl}$ generates a contraction semigroup, we apply Lumer-Phillips Theorem (Theorem 1.2.3 in [29]). The proof is done in two steps: first, we show that the operator $\mathcal{A}_{cl}$ is dissipative. Second, we show that

$$\mathrm{range}\,(\lambda I - \mathcal{A}_{cl}) \in X_s, \text{ for } \lambda > 0. \tag{43}$$

According to Definition 6.1.4 in [30], $\mathcal{A}_{cl}$ is dissipative if $\mathrm{Re}\langle \mathcal{A}_{cl}\mathcal{X}, \mathcal{X}\rangle \leq 0$, which is equivalent to $\langle \mathcal{A}_{cl}\mathcal{X}, \mathcal{X}\rangle + \langle \mathcal{X}, \mathcal{A}_{cl}\mathcal{X}\rangle \leq 0$. For the sake of clarity and without any restriction, we take $\mathcal{L}_1 = \mathcal{L}_2 = 1$ and $Q_c = I$ in the rest of this proof. From (40), one has:

$$\begin{aligned} &\langle \mathcal{A}_{cl}\mathcal{X}, \mathcal{X}\rangle + \langle \mathcal{X}, \mathcal{A}_{cl}\mathcal{X}\rangle \\ =&\langle \mathcal{G}x_2, x_1\rangle_{L_2} + \langle -\mathcal{G}^* x_1 - \mathcal{R}_{cl}x_2, x_2\rangle_{L_2} \\ &+ \langle -B_0\mathbf{1}_\zeta B_c^T x_c, x_2\rangle_{L_2} + \langle B_c\mathbf{1}_\zeta^* B_0^* x_2, x_c\rangle_{\mathbb{R}^m} \\ &+ \langle x_1, \mathcal{G}x_2\rangle_{L_2} + \langle x_2, -\mathcal{G}^* x_1 - \mathcal{R}_{cl}x_2\rangle_{L_2} \\ &+ \langle x_2, -B_0\mathbf{1}_\zeta B_c^T x_c\rangle_{L_2} + \langle x_c, B_c\mathbf{1}_\zeta^* B_0^* x_2\rangle_{\mathbb{R}^m}. \end{aligned} \tag{44}$$

According to (39), we get:

$$\begin{aligned} \langle B_0\mathbf{1}_\zeta B_c^T x_c, x_2\rangle_{L_2} &= \langle B_c\mathbf{1}_\zeta^* B_0^* x_2, x_c\rangle_{\mathbb{R}^m}, \\ \langle x_2, -B_0\mathbf{1}_\zeta B_c^T x_c\rangle_{L_2} &= \langle x_c, B_c\mathbf{1}_\zeta^* B_0^* x_2\rangle_{\mathbb{R}^m}. \end{aligned} \tag{45}$$

Substituting (45) into (44), we have:

$$\begin{aligned} &\langle \mathcal{A}_{cl}\mathcal{X}, \mathcal{X}\rangle + \langle \mathcal{X}, \mathcal{A}_{cl}\mathcal{X}\rangle \\ =&\langle \mathcal{G}x_2, x_1\rangle_{L_2} + \langle -\mathcal{G}^* x_1, x_2\rangle_{L_2} - \langle \mathcal{R}_{cl}x_2, x_2\rangle_{L_2} \\ &+ \langle x_1, \mathcal{G}x_2\rangle_{L_2} + \langle x_2, -\mathcal{G}^* x_1\rangle_{L_2} - \langle x_2, -\mathcal{R}_{cl}x_2\rangle_{L_2} \\ =&-\langle \mathcal{R}_{cl}x_2, x_2\rangle_{L_2} - \langle x_2, -\mathcal{R}_{cl}x_2\rangle_{L_2} \leq 0, \end{aligned}$$

where the last step is obtained according to the boundary conditions. Therefore, the operator $\mathcal{A}_{cl}$ is dissipative.

To show (43), we apply the proof of Theorem 3.3.6 in [31] with adjustments dedicated to our in-domain control. For the sake of simplicity, we choose $\lambda = 1$. Taking an arbitrary function

$$\mathfrak{f} = \begin{bmatrix} \tilde{x} \\ \tilde{x}_c \end{bmatrix} \in X_s,$$

(43) is then equivalent to the problem:

$$\text{find } \mathcal{X} \in X_s \text{ such that } \left(I - \mathcal{A}_{cl}\right)\mathcal{X} = \mathfrak{f}, \tag{46}$$

which is again equivalent to:

$$x_1 - \mathcal{G}x_2 = \tilde{x}_1, \tag{47a}$$
$$\mathcal{G}^* x_1 + \left(I + \mathcal{R}_{cl}\right)x_2 + B_0\mathbf{1}_\zeta B_c^T x_c = \tilde{x}_2, \tag{47b}$$
$$-B_c\mathbf{1}_\zeta^* B_0^* x_2 + x_c = \tilde{x}_c. \tag{47c}$$

Substituting (47c) into (47b), one gets:

$$\mathcal{G}^* x_1 + \left(I + \mathcal{M}\right)x_2 = \tilde{x}_2 - B_0\mathbf{1}_\zeta B_c^T \tilde{x}_c, \tag{48}$$

with $\mathcal{M} = \mathcal{R}_{cl} + B_0\mathbf{1}_\zeta B_c^T B_c \mathbf{1}_\zeta^* B_0^*$.

According to the definition of $\mathcal{G}$ and $\mathcal{G}^*$, (47a) and (48)

become:

$$x_1 - \left(G_0 + G_1 \frac{\partial}{\partial \zeta}\right) x_2 = \tilde{x}_1, \tag{49}$$

$$\left(G_0^T - G_1^T \frac{\partial}{\partial \zeta}\right) x_1 + (I + \mathcal{M})\, x_2 = \tilde{x}_f, \tag{50}$$

with $\tilde{x}_f = \tilde{x}_2 - B_0 \mathbf{1}_\zeta B_c^T \tilde{x}_c$. Thus one gets a compact form as follows:

$$\frac{\partial x}{\partial \zeta} = B_h x + g_h, \tag{51}$$

with

$$B_h = \begin{bmatrix} G_1^{-T} \begin{bmatrix} G_0^T, & I + \mathcal{M} \end{bmatrix} \\ G_1^{-1} \begin{bmatrix} 1, & -G_0 \end{bmatrix} \end{bmatrix}, \quad g_h = \begin{bmatrix} -G_1^{-T} \tilde{x}_f \\ -G_1^{-1} \tilde{x}_1 \end{bmatrix}. \tag{52}$$

The solution of the function (51) is derived as:

$$x(\zeta) = e^{B_h \zeta} x(a) + q(\zeta), \tag{53}$$

with $q(\zeta) = \int_a^\zeta e^{\zeta - s} B_h g_h \, \mathrm{d}s$.

Therefore, to solve the problem (46), one needs to find the solution of $x(\zeta)$, and eventually the solution of $x(a)$. According to the boundary condition in the domain of $\mathcal{A}_{cl}$, we have:

$$W R_{\text{ext}} \begin{bmatrix} x(b) \\ x(a) \end{bmatrix} = W R_{\text{ext}} \begin{bmatrix} e^{B_h} x(a) + q(b) \\ x(a) \end{bmatrix} = \begin{bmatrix} 0 \\ 0 \end{bmatrix}. \tag{54}$$

By calculation, $W R_{\text{ext}} \begin{bmatrix} e^{B_h} \\ I \end{bmatrix}$ has full rank. Hence, one can get the solution of $x(a)$ as:

$$x(a) = -\left(W R_{\text{ext}} \begin{bmatrix} e^{B_h} \\ I \end{bmatrix}\right)^{-1} W R_{\text{ext}} \begin{bmatrix} q(b) \\ 0 \end{bmatrix}. \tag{55}$$

Therefore $x(\zeta)$ is obtained from (53). Substituting x into (47b), one obtains x_c. As a result, the problem (46) is solved. According to the Lumer-Phillips theorem, the operator $\mathcal{A}_{cl}$ generates a contraction semigroup that concludes the proof.

Theorem 3 *The operator $\mathcal{A}_{cl}$ has a compact resolvent.*

PROOF. According to the Definition A.4.24 in [1], we need to prove that the operator $(\lambda I - \mathcal{A}_{cl})^{-1}$ is compact for some $\lambda \in \rho(\mathcal{A}_{cl})$, with $\rho(\mathcal{A}_{cl})$ denoting the resolvent set of $\mathcal{A}_{cl}$. This proof follows from Garding's inequality (Theorem 7.6.4 in [32]) and the proof of Theorem 2.26 in [33].

Define $\mathcal{T} = \lambda I - \mathcal{A}_{cl}$. From the previous Theorem 2, $\mathcal{A}_{cl}$ generates a contraction semigroup, thus $\lambda > 0$ is in the resolvent set of $\mathcal{A}_{cl}$. $\mathcal{T}$ is boundedly invertible and satisfies $\|\mathcal{T}\mathcal{X}\|_{L_2} \geq \|\mathcal{X}\|_{H^1}$. Therefore, $\mathcal{T}^{-1}$ is compact which concludes the proof.

Due to Theorem 2 and Theorem 3, the trajectory of the closed-loop system is pre-compact and its asymptotic stability can be proven by Lyapunov arguments and LaSalle's invariance principle (Theorem 3.64 of [34]) as shown in Theorem 4.

Theorem 4 *For any $\mathcal{X}(0) \in L_2\left([a,b], \mathbb{R}^{2n}\right) \times \mathbb{R}^m$, the unique solution of* (40) *tends to zero asymptotically, and the closed-loop system* (40) *is globally asymptotically stable.*

PROOF. We choose the energy of the closed-loop system as Lyapunov function. From (42), the time derivation of the Lyapunov function is semi-negative definite:

$$\frac{\mathrm{d}H_{cl}}{\mathrm{d}t} = -\int_a^b (\mathcal{L}_2 x_2)^* \mathcal{R}_{cl} (\mathcal{L}_2 x_2) d\zeta \leq 0. \tag{56}$$

Using LaSalle's invariance principle, it remains to show that the only solution associated with $\frac{\mathrm{d}H_{cl}}{\mathrm{d}t}$ is 0 *i.e.* the only solution associated with $\mathcal{L}_2 x_2 = 0$ is $x_2 = 0$. Due to the internal dissipation and zero boundary input, the only solution associated with this problem is 0. The controller being a simple integrator, if well initialized it also converges to $x_c = 0$ as the state of the system converges to $x = 0$.

4 Numerical simulations

As illustrative example we consider a vibrating string of length $L = 2$ m, modulus of elasticity $T = 1.4 \times 10^6$ N density $\rho = 1.225$ kg/m and dissipation coefficient $R = 10^{-3}$. The dynamic model of the string writes:

$$\begin{bmatrix} \dot{x}_1 \\ \dot{x}_2 \end{bmatrix} = \begin{bmatrix} 0 & \frac{\partial}{\partial \zeta} \\ \frac{\partial}{\partial \zeta} & -R \end{bmatrix} \begin{bmatrix} \mathcal{L}_1 x_1 \\ \mathcal{L}_2 x_2 \end{bmatrix} + \begin{bmatrix} 0 \\ 1 \end{bmatrix} u_d \tag{57}$$

with $x_1(\zeta, t) = \frac{\partial \omega}{\partial \zeta}(\zeta, t)$, and $x_2(\zeta, t) = \rho(\zeta) \frac{\partial \omega}{\partial t}(\zeta, t)$. $\omega(\zeta, t)$ is the longitudinal displacement over the spatial domain with the state space $x \in L_2([0, L], \mathbb{R}^2)$. $\mathcal{L}_1 = T$ and $\mathcal{L}_2 = \frac{1}{\rho}$. The dissipation term is chosen to be very

small $R = 10^{-3}$. The distributed input u_d is the force density. From Definition 1:

$$P_1 = \begin{bmatrix} 0 & 1 \\ 1 & 0 \end{bmatrix}.$$

Then the boundary port variables give:

$$\begin{bmatrix} f_\partial \\ e_\partial \end{bmatrix} = \frac{1}{\sqrt{2}} \begin{bmatrix} \mathcal{L}_2 x_2(L) - \mathcal{L}_2 x_2(0) \\ -\mathcal{L}_1 x_1(L) + \mathcal{L}_1 x_1(0) \\ \mathcal{L}_1 x_1(L) + \mathcal{L}_1 x_1(0) \\ \mathcal{L}_2 x_2(L) + \mathcal{L}_2 x_2(0) \end{bmatrix}.$$

We consider a clamped-free scenario with in-domain control. Hence, we define the boundary input formulated in (9) with:

$$W = \frac{\sqrt{2}}{2} \begin{bmatrix} 0 & 1 & 1 & 0 \\ -1 & 0 & 0 & 1 \end{bmatrix}, \quad \text{and } W \Sigma W^T \geq 0.$$

The clamped-free boundary condition implies $u_b = 0$.

The discretization matrices in (10) are:

$$J_i = \begin{bmatrix} \frac{1}{\gamma} & & & \\ -\frac{1}{\gamma^2} & \frac{1}{\gamma} & & \\ \vdots & \ddots & \ddots & \\ (-1)^{p-1} \frac{(\gamma')^{p-2}}{\gamma^p} & \cdots & -\frac{1}{\gamma^2} & \frac{1}{\gamma} \end{bmatrix}_{p \times p},$$

$B_{0d} = I_p$, $Q_1 = \text{diag}\,(T_{ab}) \in \mathbb{R}^{p \times p}$, $Q_2 = \text{diag}\left(\frac{1}{\rho_{ab}}\right) \in \mathbb{R}^{p \times p}$, $R_d = \text{diag}\,(R_{ab}) \in \mathbb{R}^{p \times p}$, with T_{ab}, $\frac{1}{\rho_{ab}}$ and R_{ab} chosen to be $\frac{T}{L_{ab}}$, $\frac{1}{\rho L_{ab}}$ and RL_{ab}, respectively. $L_{ab} = L/p$. γ denotes the effort mapping parameter [24] and $\gamma' = 1 - \gamma$. They are chosen to be $\frac{1}{2}$ in order to get a centered scheme.

Initial conditions are set to a spatial distribution $x_1(\zeta, 0) \sim \mathcal{N}(1.5, 0.113)$ for the strain distribution and to zero for the velocity distribution *i.e.*, $x_2(\zeta, 0) = 0$. The string is discretized into 50 elements. We consider a time step of 5×10^{-5}s and mid-point time discretization method [2] for simulations. The open loop evolution of the string deformation ω is given in Fig. 5.

[2] Implicit midpoint rule is known to be a structure-preserving time integration for PHSs [35]. It is a particular case in the family of symplectic collocation methods for time integration which is investigated in [25].

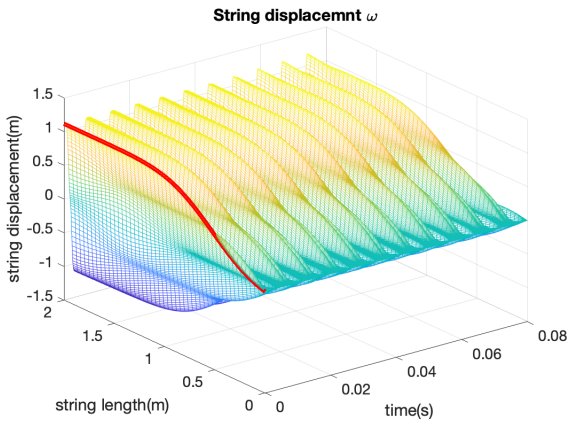

Fig. 5. Open loop deformation of the vibrating string.

Next we investigate the numerical simulations of the closed-loop system considering both fully-actuated and under-actuated cases.

4.1 Fully-actuated case

Following Proposition 1 and Proposition 2, we choose

$$B_c = \left(B_{0d}^T J_i^{-1} B_{0d}\right)^{-1} = J_i,$$

and the initial conditions of the controller such that $C = 0$. In this case (17) becomes: $x_c = x_{1d}$, and the closed-loop system (19) reads:

$$\begin{bmatrix} \dot{x}_{1d} \\ \dot{x}_{2d} \end{bmatrix} = \begin{bmatrix} 0 & J_i \\ -J_i^T & -(R_d + D_c) \end{bmatrix} \begin{bmatrix} \tilde{Q}_1 x_{1d} \\ Q_2 x_{2d} \end{bmatrix}, \tag{58}$$

One can see that *the equivalent* closed-loop stiffness $\tilde{Q}_1$ can be shaped through the choice of Q_c.

We first consider the pure damping injection, *i.e.* varying D_c with $Q_c = 0$. We consider $D_c = \text{diag}\,(\alpha L_{ab})$ with α denoting the damping coefficient. In Fig. 6(a) we can see that this degrees of freedom allows to damp the vibrations of the string to the detriment of the time response.

Next we fix $\alpha = 4000$ corresponding to the slightly over-damped case in order to illustrate the effect of the energy shaping on the achievable performances. We can see in Fig. 6(b) that we can speed up the closed-loop system by increasing the closed-loop stiffness via energy shaping, without introducing any overshoot. The energy matrix of the controller $Q_c = \text{diag}\left(\frac{\beta}{L_{ab}}\right)$, with β denoting the energy shaping parameter. A good dynamic performance is achieved when $\beta = 5 \times 10^6$, which relates to an equivalent string stiffness of $\tilde{T} = 6.4 \times 10^6$N.

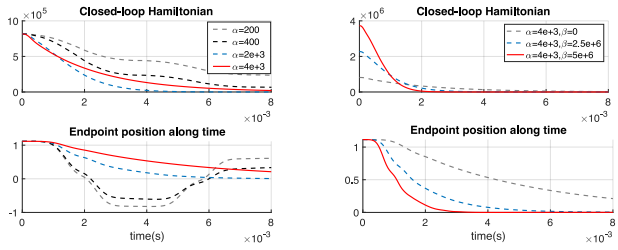

(a) (b)

Fig. 6. Closed-loop Hamiltonian function and endpoint position in the fully-actuated case with (a) pure damping injection and with (b) energy shaping plus damping injection.

The evolution of the distributed input and of the string deformation along time with damping injection and energy shaping are given in Fig. 7(a) and (b) respectively. We can see in Fig. 7(a) that the control remains smooth. Fig. 7(b) shows that the closed-loop stabilization time is about $3 \times 10^{-3}s$ which is much faster than $8 \times 10^{-3}s$ resulting from the pure damping injection case.

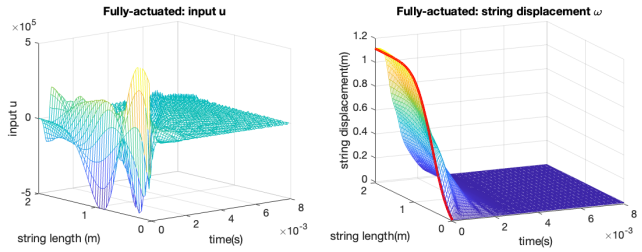

(a) (b)

Fig. 7. (a) Evolution of the closed-loop input signal and (b) deformation in the energy shaping and damping injection case with full actuation, $\alpha = 4 \times 10^3$, $\beta = 5 \times 10^6$.

4.2 Under-actuated case

We now consider that the control is achieved using m patches as depicted in Fig. 3. The aim of the control design is to modify as far as possible the internal elasticity $\tilde{T}$ of the string to get similar performances as in the fully-actuated case. We choose the controller matrix $B_c = J_m$ with $J_m \in \mathbb{R}^{m \times m}$ stemming from the discretization of $\frac{\partial}{\partial \zeta}$. According to (36) in Proposition 3, $Q_c = J_m^{-T} V \Sigma_0^{-1} U_1^T Q_m U_1 \Sigma_0^{-1} V^T J_m^{-1}$.

D_c is chosen according to Remark 2, with desired time derivative of the Hamiltonian formulated in (27) being the fully-actuated case, *i.e.* in order to satisfy $\min_{D_c \in \mathbb{R}^{m \times m}} \left\| M D_c M^T - \text{diag}\left(\alpha L_{ab}\right) \right\|_F$. As a result, the optimal D_c is given by $\hat{D}_c = \text{diag}\left(\frac{\alpha L_{ab}}{k}\right)$.

We first consider the case with 10 patches, *i.e.* $p = 50$, $m = 10$ and $k = 5$. The evolution of the string deformation as depicted in Fig. 8(a) is quite similar to that obtained in the fully-actuated case in Fig. 7(b). This indicates that if the controller matrices B_c, Q_c and D_c are adequately selected, the achievable performances in the under-actuated case can be optimized in order to be close to the ones obtained in the fully-actuated case. When the number of patches is reduced to 5, these performances are slightly deteriorated at high frequencies as shown in Fig. 8(b).

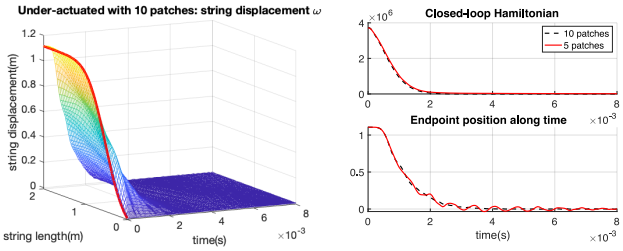

(a) (b)

Fig. 8. (a) Closed-loop evolution of the deformation with 10 patches, (b) Hamiltonian function and endpoint position in the under-actuated case for $k = 5$, and $k = 10$.

In order to illustrate the effect of the neglected dynamics on the achievable performances, we implement the controller designed considering 10 patches on the discretized system with $p = 50$, to a more precise model of the string derived using $p = 200$. In Fig. 9 we can see that, due to the damping injection and the associated closed-loop bandwidth, the neglected dynamics does not impact significantly the closed-loop response of the system to the considered initial condition. An example of in-domain controller design on Timoshenko beam model has been investigated in [22,36].

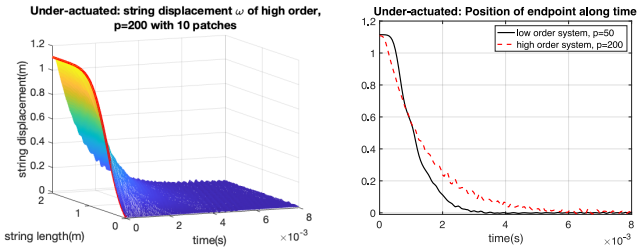

(a) (b)

Fig. 9. (a) Closed-loop evolution of the deformation of the high order system, and (b) comparison of the endpoint position of the low order and high order systems using the same controller.

5 Frequency analysis of closed-loop systems

In this section, we focus on the frequency analysis of the system. We start with the poles of the closed-loop sys-

tem with only damping injection actuated on every discretized element of the string corresponding to the simulation results in Fig. 6(a). The poles map is illustrated in Fig. 10. The damping injection puts the poles away from the imaginary axis in the left hand side of the plot, and increases the stability margin of the residual modes. Moreover, one notice that for $\alpha = 4000$, two poles of the closed-loop system are distributed on both sides of the vertical axis, as pointed out by green dashed circles. One of the poles located at -232 explains the over-damped phenomenon, which is discussed in Fig. 6(a).

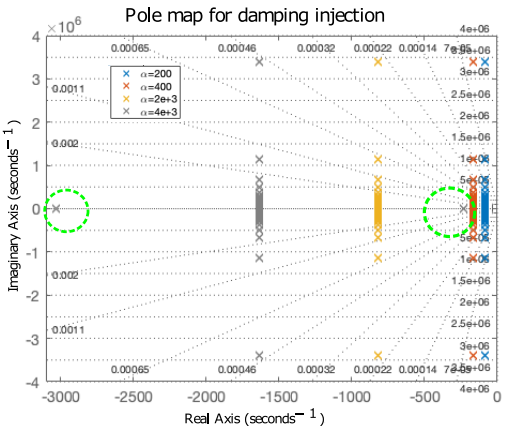

Fig. 10. Poles of the closed-loop system with damping injection for fully-actuated case.

Similarly, the poles of the closed-loop system with both the energy shaping and damping injection corresponding to Fig. 6(b) are presented in Fig. 11. The energy shaping has changed the natural frequency of the system and eliminated the aforementioned over-damping. Meanwhile, the bigger β is, the higher frequency modes appear. But the stability of the closed-loop system is always guaranteed with the damping injection.

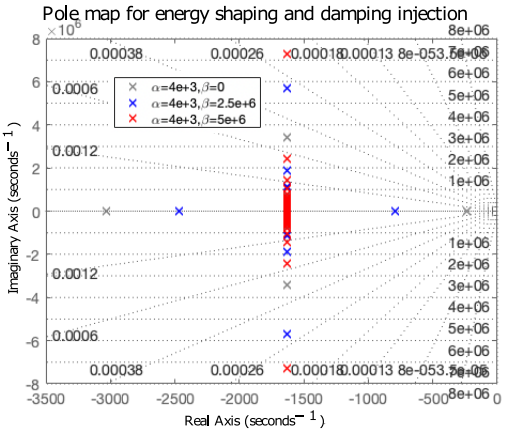

Fig. 11. Poles of the closed-loop system with energy shaping and damping injection for fully-actuated case.

For the under-actuated case as presented in Fig. 8, the poles are plotted in Fig. 12(a), with its zoom of low frequency modes in Fig. 12(b). It is shown that one can only control low frequency modes that dominate the response in order to approximate the poles distribution as in Fig. 11 for fully-actuated case. The stability of the high frequency modes, e.g. the pole $s = -0.4 \pm 3.4 \times 10^6 i$ (as pointed out by the green circle of Fig. 12(a)) of the closed-loop system with 5 patches is preserved with the internal dissipation of the string.

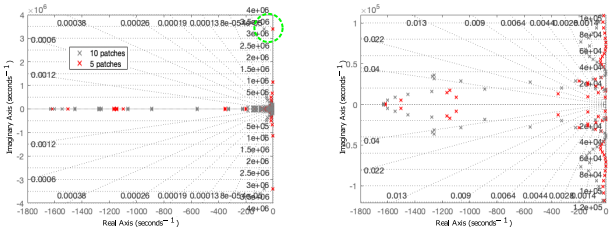

(a) (b)

Fig. 12. Poles for under-actuated case.

Remark 3 *In order to investigate the influence of damping injection to the high frequency modes in under-actuated case, we vary the matrix D_c and plot the closed-loop poles. According to Fig. 13, the conclusion is similar as the fully-actuated case presented in Fig.10.*

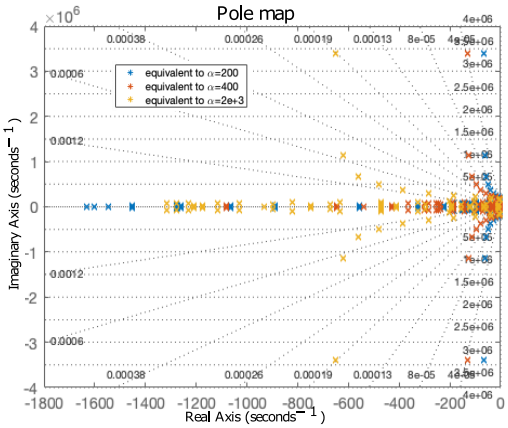

Fig. 13. Poles of the closed-loop system for under-actuated case with the change of D_c.

When the designed low order controller with 10 patches is applied to a higher order system with 200 discretized elements, the poles are presented in Fig. 14. The stability of high frequency modes is always guaranteed with the internal dissipation. If we compare the poles at low frequency modes in Fig. 14(a) with Fig. 11 and Fig. 12(a), we can notice that these poles for high order system are more away from the imaginary axis, some of which are real poles $s = -51393.5, -43073.5$ and -8658.29. These

poles have a very fast response such that they can be neglected. The zoom of high frequency poles in Fig. 14(b) are similar as in Fig. 12(a) with 10 actuator patches, which is consistent with the simulation results in Fig. 9(b).

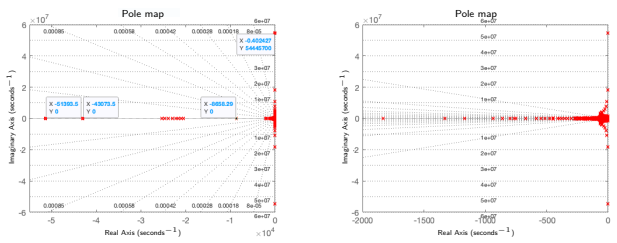

(a) (b)

Fig. 14. Poles of the high order closed-loop system ($p = 200$) with low order designed controller ($p = 50$ and $k = 10$).

6 Conclusion and future work

In this paper, we consider the in-domain control of infinite-dimensional port Hamiltonian systems with two conservation law using an early lumping approach. For control design purposes, we extend the CbI method to the use of controllers distributed in space. The distributed structural invariants are used to modify part of the closed-loop energy of the system. Two different cases are investigated: the ideal case where the system is fully-actuated and the more realistic under-actuated case where the control action is achieved using piecewise homogeneous inputs. In the latter the controller is derived by optimization. Simulations of both fully-actuated and under-actuated cases show how the damping injection together with the energy shaping improves the dynamic performances of the closed-loop system and keeps the closed-loop system asymptotically stable. Comparisons of the two cases also indicate that with an appropriate choice of the controller parameters, one can achieve similar performances for the under- and fully-actuated cases. The robustness of the proposed controller including an integrator in the closed-loop system will be investigated in the future. Future work also aims at extending the approach to the use of observers and at generalizing the proposed control design procedure to classes of non linear infinite-dimensional PHS.

References

[1] R. Curtain and H. Zwart. *An Introduction to Infinite-Dimensional Linear Systems Theory*, volume 21 of *Texts in Applied Mathematics*. Springer-Verlag New York, New York, NY, 1995.

[2] P. D. Christofides. *Nonlinear and Robust Control of PDE Systems: Methods and Applications to Transport-Reaction Processes*. Birkhäuser Boston, 2001.

[3] John A. Burns. *Nonlinear Distributed Parameter Control Systems with Non-Normal Linearizations: Applications and Approximations*, chapter 2, pages 17–53.

[4] J. L. Lions. The optimal control of distributed systems. *Russian Mathematical Surveys*, 28(4):13, aug 1973.

[5] Y. Wu, B. Hamroun, Y. Le Gorrec, and B. Maschke. Reduced order LQG control design for infinite dimensional port Hamiltonian systems. *IEEE Transactions on Automatic Control*, 66(2):865–871, 2021.

[6] I. Lasiecka and R. Triggiani. *Control Theory for Partial Differential Equations: Volume 2, Abstract Hyperbolic-Like Systems Over a Finite Time Horizon: Continuous and Approximation Theories*, volume 2. Cambridge University Press, 2000.

[7] Y. V. Orlov, A. L. Fradkov, and B. Andrievsky. Energy control of distributed parameter systems via speed-gradient method: case study of string and sine-gordon benchmark models. *International Journal of Control*, 90(11):2554–2566, 2017.

[8] Y. V. Orlov, A. L. Fradkov, and B. Andrievsky. Output feedback energy control of the sine-gordon pde model using collocated spatially sampled sensing and actuation. *IEEE Transactions on Automatic Control*, 65(4):1484–1498, 2020.

[9] V. Duindam, A. Macchelli, S. Stramigioli, and H. Bruyninckx. *Modeling and control of complex physical systems: the port-Hamiltonian approach*. Springer Science & Business Media, 2009.

[10] J. Schröck, T. Meurer, and A. Kugi. Control of a flexible beam actuated by macro-fiber composite patches: I. modeling and feedforward trajectory control. *Smart Materials and Structures*, 20(1):015015, dec 2010.

[11] N. Liu, Y. Wu, and Y. Le Gorrec. Energy based modeling of ionic polymer metal composite actuators dedicated to the control of flexible structures. *IEEE/ASME Transactions on Mechatronics*, pages 1–1, 2021.

[12] B. Maschke, A. van der Schaft, and P. Breedveld. An intrinsic Hamiltonian formulation of network dynamics: Non-standard Poisson structures and gyrators. *Journal of the Franklin institute*, 329(5):923–966, 1992.

[13] B. Maschke and A. van der Schaft. Port controlled Hamiltonian representation of distributed parameter systems. *IFAC Proceedings Volumes*, 33(2):27–37, 2000.

[14] Y. Le Gorrec, H. Zwart, and B. Maschke. Dirac structures and boundary control systems associated with skew-symmetric differential operators. *SIAM journal on control and optimization*, 44(5):1864–1892, 2005.

[15] R. Ortega, A. van der Schaft, I. Mareels, and B. Maschke. Putting energy back in control. *IEEE Control Systems Magazine*, 21(2):18–33, 2001.

[16] A. van der Schaft. *L2-Gain and Passivity Techniques in Nonlinear Control*. Springer Publishing Company, Incorporated, 3rd edition, 2016.

[17] A. Macchelli, Y. Le Gorrec, H. Ramírez, and H. Zwart. On the synthesis of boundary control laws for distributed port-Hamiltonian systems. *IEEE Transactions on Automatic Control*, 62(4):1700–1713, April 2017.

[18] V. Trenchant, T. Vu, H. Ramirez, L. Lefèvre, and Y. Le Gorrec. On the use of structural invariants for the distributed control of infinite dimensional port-Hamitonian systems. In *2017 IEEE 56th Annual Conference on Decision and Control (CDC)*, pages 47–52, Dec 2017.

[19] T. Malzer, H. Rams, and M. Schöberl. Energy-based in-domain control of a piezo-actuated Euler-Bernoulli beam.

IFAC-PapersOnLine, 52(2):144–149, 2019. 3rd IFAC Workshop on Control of Systems Governed by Partial Differential Equations CPDE 2019.

[20] T. Malzer, J. Toledo, Y. Le Gorrec, and M. Schöberl. Energy-based in-domain control and observer design for infinite-dimensional port-Hamiltonian systems. *IFAC-PapersOnLine*, 54(9):468–475, 2021. 24th International Symposium on Mathematical Theory of Networks and Systems MTNS 2020.

[21] T. Malzer, H. Rams, and M. Schöberl. On structural invariants in the energy-based in-domain control of infinite-dimensional port-Hamiltonian systems. *Systems & Control Letters*, 145:104778, 2020.

[22] N. Liu, Y. Wu, Y. Le Gorrec, L. Lefèvre, and H. Ramirez. In-domain finite dimensional control of distributed parameter port-Hamiltonian systems via energy shaping. In *2021 Proceedings of the Conference on Control and its Applications*, pages 70–77. Society for Industrial and Applied Mathematics, Philadelphia, PA, jan 2021.

[23] M. J. Balas. Toward a more practical control theory for distributed parameter systems. In C.T. LEONDES, editor, *Advances in Theory and Applications*, volume 18 of *Control and Dynamic Systems*, pages 361–421. Academic Press, 1982.

[24] G. Golo, V. Talasila, A. van der Schaft, and B. Maschke. Hamiltonian discretization of boundary control systems. *Automatica*, 40(5):757–771, 2004.

[25] P. Kotyczka, B. Maschke, and L. Lefèvre. Weak form of Stokes–Dirac structures and geometric discretization of port-Hamiltonian systems. *Journal of Computational Physics*, 361:442–476, 2018.

[26] R. Moulla, L. Lefevre, and B. Maschke. Pseudo-spectral methods for the spatial symplectic reduction of open systems of conservation laws. *Journal of computational Physics*, 231(4):1272–1292, 2012.

[27] T. Shores. *Applied linear algebra and matrix analysis*, volume 2541. Springer, 2007.

[28] N.J. Higham. Computing a nearest symmetric positive definite matrix. *Linear Algebra and its Applications*, 103:103–118, 1988.

[29] Z. Liu and S. Zheng. *Semigroups associated with dissipative systems*, volume 398. CRC Press, 1999.

[30] B. Jacob and H. Zwart. *Linear Port-Hamiltonian Systems on Infinite-dimensional Spaces*. Springer Basel, Basel, 2012.

[31] B. Augner. *Stabilisation of Infinite-Dimensional Port-Hamiltonian Systems via Dissipative Boundary Feedback*. PhD thesis, Universität Wuppertal, 2016.

[32] A.W. Naylor and G.R. Sell. *Linear Operator Theory in Engineering and Science*. Applied mathematical sciences. Holt, Rinehart and Winston, 1971.

[33] J.A. Villegas. *A Port-Hamiltonian Approach to Distributed Parameter Systems*. PhD thesis, University of Twente, 2007.

[34] Z. Luo, B. Guo, and Ö. Morgül. *Stability and stabilization of infinite dimensional systems with applications*. Springer Science & Business Media, 2012.

[35] S. Aoues, D. Eberard, and W. Marquis-Favre. Canonical interconnection of discrete linear port-Hamiltonian systems. In *2nd IEEE Conference on Decision and Control*, pages 3166–3171, 2013.

[36] Y. Le Gorrec, H. Ramirez, Y. Wu, N. Liu, and A. Macchelli. *Energy Shaping Control of 1D Distributed Parameter Systems*, pages 3–26. Springer International Publishing, Cham, 2022.